

Development of Mathematical Model of Bottom Hole Assembly for Rotary Steerable System

Ya. I. Binder¹, E.E. Kharlamova², V.E. Kharlamov³, V.P. Lozhechko⁴, V.A. Smirnov⁵ and D.A. Sokolov⁶

¹Specialnoe Konstruktorskoe Byuro Priborov Podzemnoj Navigacii, AO, St. Petersburg, Russia.

²Peter the Great St. Petersburg Polytechnic University. St. Petersburg, Russia.

³Peter the Great St. Petersburg Polytechnic University. St. Petersburg, Russia.

⁴Peter the Great St. Petersburg Polytechnic University. St. Petersburg, Russia.

⁵Specialnoe Konstruktorskoe Byuro Priborov Podzemnoj Navigacii, AO, St. Petersburg, Russia.

⁶Specialnoe Konstruktorskoe Byuro Priborov Podzemnoj Navigacii, AO, St. Petersburg, Russia.

(Corresponding author: V.P. Lozhechko)

(Received 27 September 2019, Revised 30 October 2019, Accepted 01 November 2019)

(Published by Research Trend, Website: www.researchtrend.net)

ABSTRACT: The article considers the first stage of solving the applied problem of rock destruction using modern equipment for high-precision drilling of complex profiles – Rotary Steerable Systems (RSS) of small diameter equipped with Polycrystalline Diamond Compact bits (PDC). It describes the creation of a mathematical model of the bottom hole assembly to determine the forces acting on the bit. The results of this work are applicable for further research and optimization of the process of rock-destruction with the use of the RSS.

Keywords: Bottom hole assembly, directional drilling, PDC drilling bit, push-the-bit, rotary steerable system, well trajectory.

Abbreviations: RSS, rotary steerable systems; PDC, polycrystalline diamond compact; BHA, bottom hole assembly; DU, deflecting unit.

I. INTRODUCTION

For a correct choice of a bit type, setting the operating parameters of the RSS and rock-breaking modes, it is necessary to create a model of distribution of forces and moments in the bottom hole assembly (BHA). It is known that a mechanical or hydraulic deflecting mechanism serves as a control element of the RSS, providing the intensity of the spatial curvature of the well. The principle of operation of the deflecting mechanism determines the technology and type of the system [1-3]. Push-the-bit technology is based on the deviation of the entire assembly or most of it by pushing away from the wellbore wall. Obviously, as a result of such an impact, the drilling assembly receives a deflection, and the tool is located in the well with some tilt. Thus, a lateral force appears, directed from the axis of the drilling tool in the direction of the wellbore wall, and, as a result, the bit begins to mill the wellbore wall, and the intensity of this process mainly determines the lateral cutting structure of the bit.

It should be noted that the process of such interaction of the bit and the wellbore wall, in the case of using RSS, has not been well studied. Apparently this research gap is connected to the fact that current study is at the junction of two areas - the classical theory of well drilling and studies related to the analysis of the work of the relatively new and complex technology - RSS. To optimize the drilling mode it is necessary to have a precise understanding of the mechanics of the cutting-spalling processes that occur in such conditions.

II. METHODOLOGY

Let us consider the mechanism of curvature of the wells and the main causes of the uneven destruction of rock

at the bottom of a well. Each of these causes manifests itself in the form of forces and pull-out moments acting on the rock-breaking tool. All these forces and moments can be reduced to one resultant force and resultant moment. In this case, four variants are possible (Fig. 1).

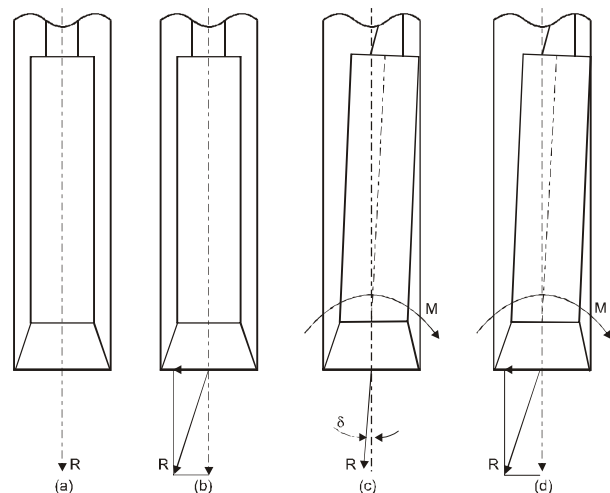


Fig. 1. The mechanism of wells curvature.

1. All the operating forces come down to the resultant one, coinciding with the axis of the bit, the moment is absent Fig. 1 (a). In this case, drilling of a straight well is provided. Thus, if the curvature is undesirable, it is necessary to create the above conditions, which, however, is difficult to achieve [1, 4, 5, 6].

2. All the operating forces are reduced to the resultant, coinciding with the axis of the bit, the moment is absent Fig. 1 (b). At the same time, under the action of the lateral component of this force, the bit is pressed

against the wall of the borehole and mills it in the process of drilling. In this case, the well curvature occurs only due to the milling of the borehole wall with intensity depending on the geometric dimensions and elastic deformation of the BHA guide section, the bore diameter, physical and mechanical properties of the rocks composing the wellbore wall, the specific contact load on them and the lateral milling capacity of the bit, as well as the mechanical penetration rate. And the maximum intensity of the curvature of the bore hole depends on the geometric dimensions and the elastic deformation of the guide section of the BHA and the diameter of the well.

It should be noted that with the curvature only due to the milling of the wellbore wall, there are sharp bends in the bore hole, which leads to the jamming of the tool during the descent and requires additional reaming of the well.

3. All existing forces are reduced to the resultant, coinciding with the axis of the bit and to a pair of forces, the moment of which is equal to the resultant moment of all forces relative to the center of the bit Fig. 1 (c). As a result, a certain angle δ is formed between the axis of the well and the axis of the tool. In this case, the curvature of the well occurs without milling the hole wall as a result of the inclined position of the bit relative to the axis of the well. The peculiarity of such a curvature is that it does not depend on the mechanical penetration rate and lateral milling capacity of the bit, and the physical and mechanical properties of the drilled rocks have an indirect effect only by changing the diameter of the well and introducing elements of the BHA guide section into the bore hole wall. The well axis is a smooth line close to the arc of a circle, which facilitates all subsequent work. And the maximum intensity of the curvature of the hole depends on its diameter, geometric dimensions and the elastic deformation of the guide section of the BHA.

4. All existing forces come down to the resultant, coinciding with the axis of the bit and to a pair of forces, the moment of which is equal to the resultant moment of all forces relative to the center of the bit Fig. (d). In this case, the curvature of the well occurs without milling the bore hole wall as a result of the inclined position of the bit relative to the axis of the well. At the same time, the intensity of the bore hole curvature will be affected by the factors characterizing the physical and mechanical properties of the drilled rocks, the deflecting force on the bit, the lateral milling capacity and the contact area of the bit, the well diameter, the geometric dimensions and the condition of the BHA guideline. The maximum intensity of the hole curvature in this case will depend on the fit of the specified section of the BHA into the bore hole, i.e. on the bore hole diameter, the geometric dimensions and the elastic deformation of this area [7]. Obviously, the last two cases are of the greatest interest. The third case is preferable in terms of obtaining the well profile optimal from the point of view of further exploitation; however, it is possible only with the use of the "Point-the-Bit" bit turning technology and therefore is not considered in this paper.

The fourth case relates directly to the systems using the "Push-the-bit" bit displacement technology, in which lateral force arises as a result of repulsion of the BHA deflecting element from the wellbore wall, and the inclined position of the bit relative to the well axis is due

to the elastic deformation of the BHA guide section impacted by a deflecting effort.

The well deepening process is characterized by low (50 m/h or less) drilling rates, so if you aim to study the behavior of a drilling tool designed to fulfill the projected profile of a well, and solve the problem of optimizing its parameters accordingly, so it is enough to choose correctly the criterion of its optimization, static design scheme and the analytical model of the diverter or BHA corresponding to it.

In consequence of the foregoing in order to analyze the process of destruction of drilled rocks, it is necessary to investigate the dependence of elastic deformations of a BHA depending on its geometrical parameters.

According to [7], in an inclined well of rectilinear forms there is no equilibrium at all in the lower part of the BHA. Therefore, when designing the BHA for directional drilling, recommendations on the choice of stiffness and linear parameters developed for vertical drilling cannot be used based on the concept of stability of the drill string.

To determine the forces and moments arising at the bottom hole and acting on the BHA with rotary steerable drilling, it is necessary to calculate the curving scheme of the "Push-the-Bit" BHA shown in Fig. 2.



Fig. 2. BHA with RSS.

1 - Upper stabilizer, 2 - flexible insert, 3 - lower stabilizer, 4 - rotary steerable system, 5 - deflecting shoes, 6 - rock cutting tool (bit).

In the assemblies of this type, the stabilizers, relying on the walls of the well, play the role of supporting points (hinge joints) and allow the BHA to bend in the right direction. Basically, the deflection is carried out due to the flexible insert, which has a lower flexural and torsional stiffness. This type of the assembly was investigated in [1, 7, 8]. However, for use in this work, the previously studied scheme is not applicable for the following reasons:

- In papers [1, 7], the RSS without a deflecting unit was considered, therefore, there is only one point of application of the deflecting radial force to the BHA. In the RSS with a geostationary deflecting unit, the deflecting shoes are located on it, and, as a result, there are two points of application of the deflecting radial force.

- In the assemblies with a geostationary deflecting unit, the shaft transmitting torque and axial force to the bit freely passes through the RSS and has a smaller cross-section than the RSS itself. For this reason, its bend cannot be neglected.

In addition to the above reasons, previous studies do not take into account:

- The position of the BHA in space, in particular the directions of gravity, etc.

- The influence of the geometric and mechanical parameters of the flexible insert and drill pipes above the lower stabilizer on the angles of rotation was not studied analytically. The BHA should be designed as a continuous beam, taking into account that the supports are not located on the same straight line.

– The variable rigidity of the assembly is not taken into account, due to the change in the cross section of the BHA.

Further, we will consider in more detail the BHA, which includes a RSS with a geostationary Deflecting Unit (DU) and using the “push-the-bit” bit shift technology (Fig. 3).



Fig. 3. BHA with geostationary DU.

1- bit, 2- radial bearing unit, 3- deflecting shoes, 4- radial-thrust bearing unit, 5- lower stabilizer, 6- upper stabilizer.

Further we will use the following notation:

- Point A- the point of intersection of the BHA centerline and the bit face.
- Point B- the point of intersection of the BHA centerline and the radial bearing installation plane.
- Point C is the point of intersection of the BHA centerline and the plane of installation of the radial-thrust bearings.
- Point D is the point of intersection of the BHA centerline and the mid-plane of the calibrating area of the lower stabilizer.
- Point E is the intersection point of the BHA centerline and mid-plane of the calibrating area of the upper stabilizer.

As can be seen from Fig. 2, DU of the RSS is unleashed from rotation of the drill string with the help of two bearing units, one of which is made radial, and the second radial-thrust. Thus, when the deflecting shoe is pressed against the wellbore wall, the radial force will be transmitted to the shaft with a value inversely proportional to the shoulders of these forces relative to the point of contact with the wellbore wall. It should also be noted that during the DU movement in the well, in the axial direction, friction force inevitably arises, to determine the magnitude of which a separate study is required. In the framework of this study, it is assumed that the resultant force is directed along the DU axis and is applied at point C.

Then, to calculate the transmitted effort, the scheme shown in Fig. 4 will be valid.

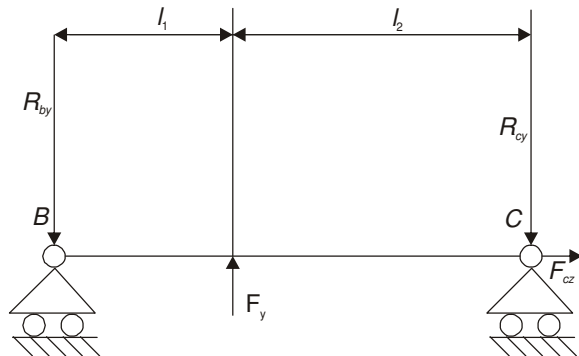


Fig. 4. DU deflecting efforts scheme.

l_1 - the distance from the radial bearing unit to the deflecting shoe, l_2 - the distance from the radial-thrust bearing unit to the deflecting shoe, R_{by} - reaction force

arising in the radial bearing, R_{cy} - reaction force arising in a radial-thrust bearing, F_y - the force created by the deflecting shoe

Let's create a system of statics equations for this scheme:

$$\begin{cases} F_y \times l_1 - R_{cy} \times (l_1 + l_2) = 0 \\ F_y - R_{by} - R_{cy} = 0 \\ R_{cy} = \frac{F_y \times l_1}{(l_1 + l_2)} \\ R_{by} = F_y - R_{cy} \end{cases} \quad (1)$$

Further, we will consider the reaction forces as known quantities and proceed to the consideration of the BHA scheme. To do this, assume that the DU doesn't bend, and the BHA under the action of a force F_y , bends in the apsidal plane along an arc of a circle of a radius R and a center at the point O, as shown in Fig. 5. At the same time, the bit is fixed with the hinges, since, according to [9], there is no analogue of the hinge fixing of the end of the drill string in any inclined well at any length of the BHA.

R_{ay}, R_{az} - support reactions at point A along the y and z axes, respectively, R_{do}, R_{eo} - reaction of supports at points D and E in the direction of the center of the trajectory curvature, F_e - axial force F_b, F_c - deflecting forces transmitted through the bearing units, α_{bc} - the angle of inclination of the deflecting unit relative to the axis Z, q_1 and q_2 - distributed load, based on the weight of BHA itself

The hinge condition of the bit fixing is necessary to determine the radial and axial component of the resultant force at point A. Obviously, the section AB in Fig. 5 must be straight or close to it, since this is the area between the bit and the radial bearing assembly. However, during the calculation this straightness will not be taken into account, since its length is comparatively small, and will lead to an additional complication of the task. The distributed load acting on the BHA cannot be accurately determined along a circular arc; therefore, its average value in the middle of the studied area will be accepted, and the section itself will be considered straightforward. Let's divide the entire BHA into 2 sections, one of which is a part from the cutting area of the bit to the lower stabilizer, and the second is the section between the lower and upper stabilizers. This system is statically indefinable, since it contains 4 unknown reactions, and can be attributed to continuous multi-support beams. To solve such problems, the three-moment equation is widely used; however, it does not take into account the variable stiffness of the beam. In order to take into account the stiffness of such a beam, it is necessary to use the method of forces, having previously calculated each of the two parts as a separate compressed-bent beam with a fore-aft bend. Despite its cumbersomeness, this solution will be the only one as close as possible to the real picture. To simplify the solution and reduce the number of design intervals, we will assume that the change in the cross section of the shaft of the RSS takes place directly at the installation points of the bearing units. Then each beam is divided into 3 intervals of different stiffness. Thus, the design scheme takes the form shown in Fig. 6.

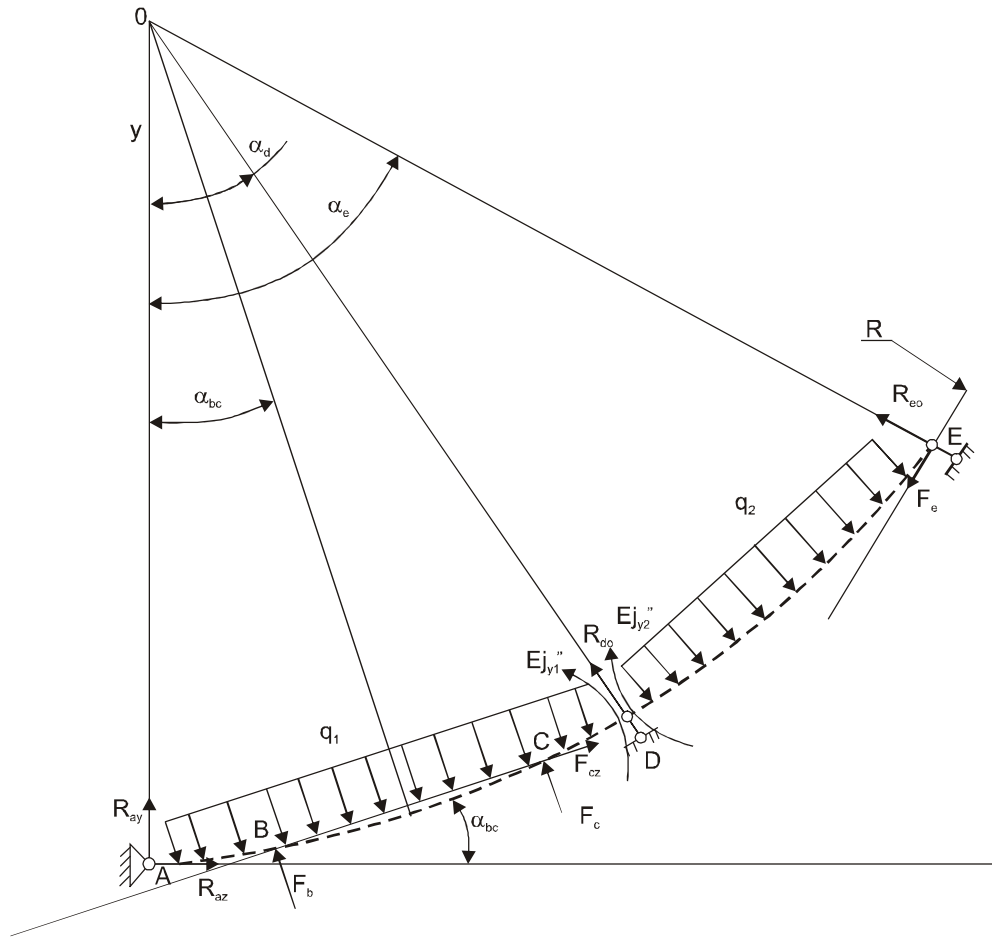


Fig. 5. BHA with RSS analytical model.

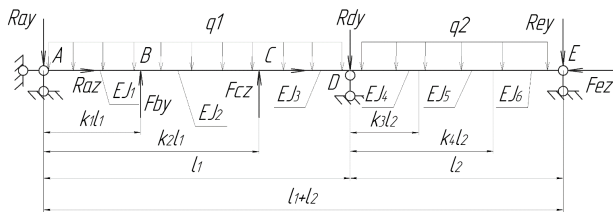


Fig. 6. The design scheme of the continuous beam for the BHA.

Since the resulting beam is statically indefinable, it is necessary to remove redundant constraints and consider two statically definable systems. To do this, let's cut the beam at point D and apply the bending moment of the mutual influence of the beams on each other X to both parts. The equivalent basic system thus obtained is shown in Fig. 7.

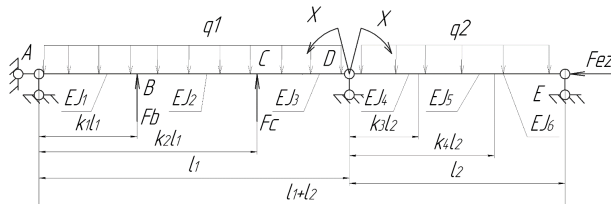


Fig. 7. Equivalent system.

To determine the moment X at point D, it is necessary to calculate two two-support statically definable systems with all applied loads. In the case of longitudinal-transverse bending, the principle of independence of the action of forces is not applicable, since transverse bending arising from the action of radial forces is enhanced by the action of axial load. However, it is possible to calculate the effect of axial load on each transverse force and present the total deflection as an algebraic sum of the results. This will avoid cumbersome solutions, and trace the influence of the longitudinal force on each component separately [10-12].

As a result of calculations for the first beam, the following results were obtained:

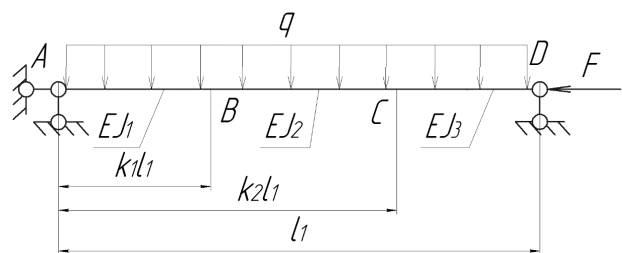


Fig. 8. Distributed load.

$$\begin{cases} y_1 = C_1 \times \cos(\alpha_1 \times z) + C_2 \times \sin(\alpha_1 \times z) + \frac{q}{2 \times F} \times z^2 - \frac{q \times l_1}{2 \times F} \times z - \frac{q \times E \times J_1}{F^2}, \text{ where } 0 < z < k1l \\ y_2 = C_3 \times \cos(\alpha_2 \times z) + C_4 \times \sin(\alpha_2 \times z) + \frac{q}{2 \times F} \times z^2 - \frac{q \times l_1}{2 \times F} \times z - \frac{q \times E \times J_2}{F^2}, \text{ where } k1l < z < k2l, \\ y_3 = C_5 \times \cos(\alpha_3 \times z) + C_6 \times \sin(\alpha_3 \times z) + \frac{q}{2 \times F} \times z^2 - \frac{q \times l_1}{2 \times F} \times z - \frac{q \times E \times J_3}{F^2}, \text{ where } k2l < z < l \end{cases} \quad (2)$$

where α_j - is equal to:

$$\alpha_j = \sqrt{\frac{F}{EJ_j}},$$

and C_n - constants of integration of the differential equation of the curved beam axis, determined by solving a system of 6 equations obtained by substituting the boundary conditions of the problem.

Before this, you should make some change of variables used in the future:

$$\left\{ \begin{array}{l} f(X_{ji}) = f(\alpha_j, k_i, l) \\ f(X_{j0}) = f(\alpha_j, l) \\ w_1 = \alpha_2 \times \sin(X_{21}) + \alpha_1 \times ctg(X_{11}) \times \cos(X_{21}) \\ w_2 = tg(X_{32}) \times \frac{(tg(X_{30}) + ctg(X_{32}))}{(tg(X_{32}) - tg(X_{30}))} \\ w_3 = \alpha_3 \times w_2 \times \cos(X_{22}) + \alpha_2 \times \sin(X_{22}) \\ w_4 = \alpha_2 \times \cos(X_{22}) - \alpha_3 \times w_2 \times \sin(X_{22}) \\ w_5 = \alpha_2 \times \cos(X_{21}) - \alpha_1 \times ctg(X_{11}) \times \sin(X_{11}) \\ w_6 = \alpha_3 \times \left(J_3 \times \frac{\sin(X_{32})}{\cos(X_{30})} - w_2 \times \left(J_3 \times \left(1 - \frac{\cos(X_{32})}{\cos(X_{30})} - J_2 \right) \right) \right) \\ w_7 = \alpha_1 \times (J_1 \times \sin(X_{11}) - ctg(X_{11}) \times (J_1 \times (1 - \cos(X_{11}) - J_2))) \end{array} \right. \quad (3)$$

In view of (3), constants C_n will have the following form:

$$\left\{ \begin{array}{l} C_1 = \frac{q \times E}{F^2} \times J_1 = \frac{q \times E}{F^2} \times \beta_1^p \\ C_4 = \frac{q \times E}{F^2} \times \left(\frac{\frac{w_6}{w_3} \frac{w_7}{w_4}}{\frac{w_1}{w_2} \frac{w_3}{w_4}} \right) = \frac{q \times E}{F^2} \times \beta_4^p \\ C_3 = \frac{q \times E}{F^2} \times \left(\frac{\frac{w_6}{w_3} \frac{w_7}{w_4}}{\frac{w_1}{w_2} \frac{w_3}{w_4}} + \frac{w_6}{w_3} \right) = \frac{q \times E}{F^2} \times \beta_3^p \\ C_2 = \frac{q \times E}{F^2} \times (J_1 \times tg(X_{11}) + \frac{\alpha_2}{\alpha_1 \times \cos(X_{11})} \times (\beta_4^p \times \cos(X_{21}) - \beta_3^p \times \sin(X_{21}))) = \frac{q \times E}{F^2} \times \beta_2^p \\ C_6 = \frac{q \times E}{F^2} \times \left(\frac{\alpha_2}{\alpha_3 \times (tg(X_{30}) \times \sin(X_{32}) + \cos(X_{32}))} \times (\beta_4^p \times \cos(X_{22}) - \beta_3^p \times \sin(X_{22})) + J_3 \frac{\alpha_3 \times \sin(X_{32})}{\alpha_2 \times \cos(X_{30})} \right) = \frac{q \times E}{F^2} \times \beta_6^p \\ C_5 = \frac{q \times E}{F^2} \times \left(\frac{J_3 - \beta_6^p \times \sin(X_{30})}{\cos(X_{30})} \right) = \frac{q \times E}{F^2} \times \beta_5^p \end{array} \right. \quad (4)$$

From Eqns. (2), (3) and (4) it can be seen that all the factors in the equations of the diagram axis are decomposed into independent of the axial load, directly related to it.

Thus, for the moment X (Fig. 7), the solution will be as follows:

$$\begin{cases} y_1 = C_1 \times \cos(\alpha_1 \times z) + C_2 \times \sin(\alpha_1 \times z) - \frac{M}{l \times F} \times z, \text{ where } 0 < z < k1l \\ y_2 = C_3 \times \cos(\alpha_2 \times z) + C_4 \times \sin(\alpha_2 \times z) - \frac{M}{l \times F} \times z, \text{ where } k1l < z < k2l \\ y_3 = C_5 \times \cos(\alpha_3 \times z) + C_6 \times \sin(\alpha_3 \times z) - \frac{M}{l \times F} \times z, \text{ where } k2l < z < l \end{cases} \quad (5)$$

where,

$$\left\{ \begin{array}{l} w_9 = \frac{\alpha_3 \times \sin(X_{32}) + \alpha_3 \times w_2 \times \cos(X_{32})}{\cos(X_{30})} \\ C_1 = 0 \\ C_4 = \frac{M}{F} \times \left(\frac{\frac{w_9}{w_3}}{\frac{w_1}{w_2} \frac{w_3}{w_4}} \right) = \frac{M}{F} \times \beta_4^{X1} \\ C_3 = \frac{M}{F} \times \left(\beta_4^{X1} \times \frac{w_5}{w_1} \right) = \frac{M}{F} \times \beta_3^{X1} \\ C_2 = \frac{M}{F} \times \left(\frac{1}{\sin(X_{11})} \times (\beta_3^{X1} \times \cos(X_{21}) + \beta_4^{X1} \times \sin(X_{21})) \right) = \frac{M}{F} \times \beta_2^{X1} \\ C_6 = \frac{M}{F} \times \left(\frac{1}{tg(X_{32}) - tg(X_{30})} \times (\beta_3^{X1} \times \frac{\cos(X_{22})}{\cos(X_{32})} + \beta_4^{X1} \times \frac{\sin(X_{22})}{\cos(X_{32})} - \frac{1}{\cos(X_{30})}) \right) = \frac{M}{F} \times \beta_6^{X1} \\ C_5 = \frac{M}{F} \times \left(\frac{1}{\cos(X_{30})} - \beta_6^{X1} \times tg(X_{30}) \right) = \frac{M}{F} \times \beta_5^{X1} \end{array} \right. \quad (6)$$

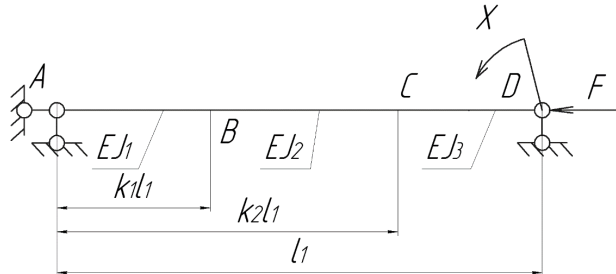


Fig.9. The moment applied on the support D.

However, for the concentrated load of Fig.10, the separation of variables is not observed, due to the different possible ratio of forces applied at points B and C:

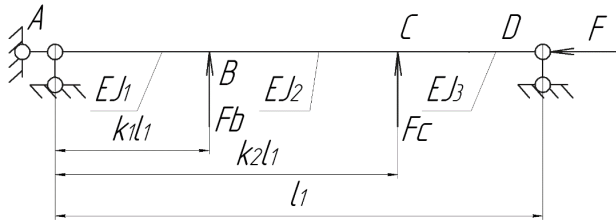


Fig.10. Concentrated load.

$$\begin{cases} y_1 = C_1 \times \cos(\alpha_1 \times z) + C_2 \times \sin(\alpha_1 \times z) - \frac{F_b \times (1-k_1) + F_c \times (1-k_2)}{F} \times z, \text{ where } 0 < z < k_1 l_1 \\ y_2 = C_3 \times \cos(\alpha_2 \times z) + C_4 \times \sin(\alpha_2 \times z) + \frac{F_b \times k_1 + F_c \times (k_2 - 1)}{F} \times z - \frac{F_b \times k_1 \times l_1}{F}, \text{ where } k_1 l_1 < z < k_2 l_1 \\ y_3 = C_5 \times \cos(\alpha_3 \times z) + C_6 \times \sin(\alpha_3 \times z) + \frac{F_b \times k_1 + F_c \times k_2}{F} \times z - \frac{F_b \times k_1 + F_c \times k_2}{F} \times l_1, \text{ where } k_2 l_1 < z < l_1 \end{cases} \quad (7)$$

where,

$$\begin{cases} C_1 = 0 \\ C_4 = \frac{1}{F} \times \left(\frac{F_c \times w_1 + F_b \times w_3}{\left(\frac{w_5}{w_1} - \frac{w_4}{w_3} \right) \times w_3 \times w_1} \right) = \frac{1}{F} \times \beta_4^c \\ C_3 = \frac{1}{F} \times \left(\beta_4^c \times \frac{w_4}{w_3} - \frac{F_c}{w_3} \right) = \frac{1}{F} \times \beta_3^c \\ C_2 = \frac{1}{F} \times \left(\frac{1}{\sin(X_{11})} \times \left(\beta_3^c \times \cos(X_{21}) + \beta_4^c \times \sin(X_{21}) \right) \right) = \frac{1}{F} \times \beta_2^c \\ C_6 = \frac{1}{F} \times \left(\frac{1}{\operatorname{tg}(X_{32}) - \operatorname{tg}(X_{30})} \times \left(\beta_3^c \times \frac{\cos(X_{22})}{\cos(X_{32})} + \beta_4^c \times \frac{\sin(X_{22})}{\cos(X_{32})} - \frac{1}{\cos(X_{30})} \right) \right) = \frac{1}{F} \times \beta_6^c \\ C_5 = \frac{1}{F} \times \left(\frac{1}{\cos(X_{30})} - \beta_6^c \times \operatorname{tg}(X_{30}) \right) = \frac{1}{F} \times \beta_5^c \end{cases} \quad (8)$$

For the second beam corresponding to the flexible insert, the expressions for calculating the distributed load fully correspond to (2) and (4).

However, to calculate the deflection caused by the bending moment X, another scheme is required (Fig. 11).

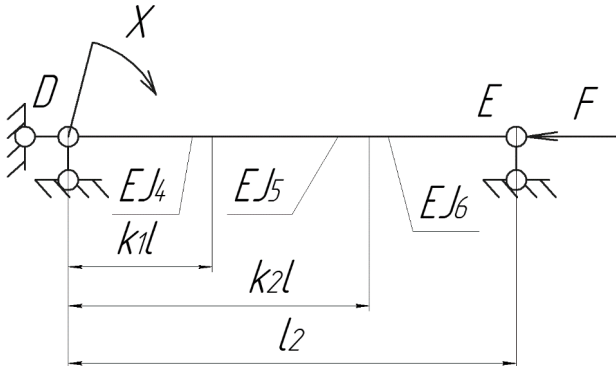


Fig.11. The moment applied on the support D.

$$\begin{cases} y_1 = C_1 \times \cos(\alpha_1 \times z) + C_2 \times \sin(\alpha_1 \times z) + \frac{X}{l \times F} \times z - \frac{X}{F}, \text{ where } 0 < z < k1l \\ y_2 = C_3 \times \cos(\alpha_2 \times z) + C_4 \times \sin(\alpha_2 \times z) + \frac{X}{l \times F} \times z - \frac{X}{F}, \text{ where } k1l < z < k2l \\ y_3 = C_5 \times \cos(\alpha_3 \times z) + C_6 \times \sin(\alpha_3 \times z) + \frac{X}{l \times F} \times z - \frac{X}{F}, \text{ where } k2l < z < l \end{cases} \quad (9)$$

$$\begin{cases} w_8 = \alpha_1 \times \frac{1}{\sin(X_{11}) \times w_1} \\ C_1 = \frac{X}{F} \\ C_4 = \frac{X}{F} \times \left(\frac{w_8}{\frac{w_4}{w_3} \cdot \frac{w_5}{w_1}} \right) = \frac{X}{F} \times \beta_4^{X^2} \\ C_3 = \frac{X}{F} \times \left(\beta_4^{X^2} \times \frac{w_4}{w_3} \right) = \frac{X}{F} \times \beta_3^{X^2} \\ C_2 = \frac{X}{F} \times \left(\frac{1}{\sin(X_{11})} \times (\beta_3^{X^2} \times \cos(X_{21}) + \beta_4^{X^2} \times \sin(X_{21}) - \cos(X_{11})) \right) = \frac{X}{F} \times \beta_2^{X^2} \\ C_6 = \frac{X}{F} \times \left(\frac{1}{\cos(X_{32}) \times (tg(X_{32}) - tg(X_{30}))} \times (\beta_3^{X^2} \times \cos(X_{22}) + \beta_4^{X^2} \times \sin(X_{22})) \right) = \frac{X}{F} \times \beta_6^{X^2} \\ C_5 = \frac{X}{F} \times \left(-\beta_6^{X^2} \times tg(X_{30}) \right) = \frac{X}{F} \times \beta_5^{X^2} \end{cases} \quad (10)$$

According to the method of forces, solving the canonical equation of the form

$$X \times \delta_{11} + \delta_{1F} = 0 \quad (11)$$

where,

$$\delta_{11} = \frac{M_1 \times M_1}{EJ} \quad (12)$$

$$\delta_{1F} = \frac{M_1 \times M_F}{EJ} \quad (13)$$

the moment X is determined on support E. Knowing the value of this moment, with different input parameters, it is possible to make common for both beams diagrams of deflections, angles of rotation of the cross section, bending moment, and also calculate the reactions on all the supports. This is especially important for studying the interaction of the bit and borehole stabilizers with the wellbore walls. Knowing all the parameters of their location in the well, it is possible to qualitatively estimate the magnitude of the forces and moments of friction, and, therefore, optimize the layout in terms of the effectiveness of maintaining a given direction of drilling.

In order to multiply one diagram by another, it is necessary to determine the coordinate along the Z axis of the center of mass of a certain interval and multiply the value of the diagram in this coordinate by the value of the second diagram in the corresponding coordinate [13-15].

Since all equations for these diagrams are obtained in an analytical form, and the diagrams do not correspond to standard and simple geometric figures, to calculate the center of mass, it is necessary to determine the moment of inertia along the x axis and the area interval, and then divide the area by the moment of inertia.

For a distributed load, Eqn. (2) will take the form:

$$\begin{cases} y_1 = C_1 \times \cos(\alpha_1 \times z) + C_2 \times \sin(\alpha_1 \times z) + \frac{q}{2 \times F} \times z^2 - \frac{q \times l_1}{2 \times F} \times z - \frac{q \times E \times J_1}{F^2}, \text{ where } 0 < z < k1l \\ y_1' = C_2 \times \alpha_1 \times \cos(\alpha_1 \times z) - C_1 \times \alpha_1 \times \sin(\alpha_1 \times z) + \frac{q}{F} \times z - \frac{q \times l}{2 \times F} \\ y_1'' = -C_1 \times \alpha_1^2 \times \cos(\alpha_1 \times z) - C_2 \times \alpha_1^2 \times \sin(\alpha_1 \times z) + \frac{q}{F} \\ y_2 = C_3 \times \cos(\alpha_2 \times z) + C_4 \times \sin(\alpha_2 \times z) + \frac{q}{2 \times F} \times z^2 - \frac{q \times l_1}{2 \times F} \times z - \frac{q \times E \times J_2}{F^2}, \text{ where } k1l < z < k2l \\ y_2' = C_4 \times \alpha_2 \times \cos(\alpha_2 \times z) - C_3 \times \alpha_2 \times \sin(\alpha_2 \times z) + \frac{q}{F} \times z - \frac{q \times l}{2 \times F} \\ y_2'' = -C_3 \times \alpha_2^2 \times \cos(\alpha_2 \times z) - C_4 \times \alpha_2^2 \times \sin(\alpha_2 \times z) + \frac{q}{F} \\ y_3 = C_5 \times \cos(\alpha_3 \times z) + C_6 \times \sin(\alpha_3 \times z) + \frac{q}{2 \times F} \times z^2 - \frac{q \times l_1}{2 \times F} \times z - \frac{q \times E \times J_3}{F^2}, \text{ where } k2l < z < l \\ y_3' = C_6 \times \alpha_3 \times \cos(\alpha_3 \times z) - C_5 \times \alpha_3 \times \sin(\alpha_3 \times z) + \frac{q}{F} \times z - \frac{q \times l}{2 \times F} \\ y_3'' = -C_5 \times \alpha_3^2 \times \cos(\alpha_3 \times z) - C_6 \times \alpha_3^2 \times \sin(\alpha_3 \times z) + \frac{q}{F} \end{cases} \quad (14)$$

For a concentrated load, Eqn. (5) will take the form:

$$\left\{ \begin{array}{l} y_1 = C_1 \times \cos(\alpha_1 \times z) + C_2 \times \sin(\alpha_1 \times z) - \frac{F_b \times (1-k_1) + F_c \times (1-k_2)}{F} \times z, \text{ where } 0 < z < k1l \\ y_1' = C_2 \times \alpha_1 \times \cos(\alpha_1 \times z) - C_1 \times \alpha_1 \times \sin(\alpha_1 \times z) - \frac{F_b \times (1-k_1) + F_c \times (1-k_2)}{F} \\ y_1'' = -C_1 \times \alpha_1^2 \times \cos(\alpha_1 \times z) - C_2 \times \alpha_1^2 \times \sin(\alpha_1 \times z) \\ y_2 = C_3 \times \cos(\alpha_2 \times z) + C_4 \times \sin(\alpha_2 \times z) + \frac{F_b \times k_1 + F_c \times (k_2-1)}{F} \times z - \frac{F_b \times k_1 \times l}{F}, \text{ where } k1l < z < k2l \\ y_2' = C_4 \times \alpha_2 \times \cos(\alpha_2 \times z) - C_3 \times \alpha_2 \times \sin(\alpha_2 \times z) + \frac{F_c \times (k_2-1) + F_b \times k_1}{F} \\ y_2'' = -C_3 \times \alpha_2^2 \times \cos(\alpha_2 \times z) - C_4 \times \alpha_2^2 \times \sin(\alpha_2 \times z) \\ y_3 = C_5 \times \cos(\alpha_3 \times z) + C_6 \times \sin(\alpha_3 \times z) + \frac{F_b \times k_1 + F_c \times k_2}{F} \times z - \frac{F_b \times k_1 + F_c \times k_2}{F} \times l, \text{ where } k2l < z < l \\ y_3' = C_6 \times \alpha_3 \times \cos(\alpha_3 \times z) - C_5 \times \alpha_3 \times \sin(\alpha_3 \times z) + \frac{F_b \times k_1 + F_c \times k_2}{F} \\ y_3'' = -C_5 \times \alpha_3^2 \times \cos(\alpha_3 \times z) - C_6 \times \alpha_3^2 \times \sin(\alpha_3 \times z) \end{array} \right. \quad (15)$$

For the moment on support D attached to the first beam, Eqn. (7) will take the form:

$$\left\{ \begin{array}{l} y_1 = C_1 \times \cos(\alpha_1 \times z) + C_2 \times \sin(\alpha_1 \times z) - \frac{M}{l \times F} \times z, \text{ where } 0 < z < k1l \\ y_1' = C_2 \times \alpha_1 \times \cos(\alpha_1 \times z) - C_1 \times \alpha_1 \times \sin(\alpha_1 \times z) - \frac{M}{l \times F} \\ y_1'' = -C_1 \times \alpha_1^2 \times \cos(\alpha_1 \times z) - C_2 \times \alpha_1^2 \times \sin(\alpha_1 \times z) \\ y_2 = C_3 \times \cos(\alpha_2 \times z) + C_4 \times \sin(\alpha_2 \times z) - \frac{M}{l \times F} \times z, \text{ where } k1l < z < k2l \\ y_2' = C_4 \times \alpha_2 \times \cos(\alpha_2 \times z) - C_3 \times \alpha_2 \times \sin(\alpha_2 \times z) - \frac{M}{l \times F} \\ y_2'' = -C_3 \times \alpha_2^2 \times \cos(\alpha_2 \times z) - C_4 \times \alpha_2^2 \times \sin(\alpha_2 \times z) \\ y_3 = C_5 \times \cos(\alpha_3 \times z) + C_6 \times \sin(\alpha_3 \times z) - \frac{M}{l \times F} \times z, \text{ where } k2l < z < l \\ y_3' = C_6 \times \alpha_3 \times \cos(\alpha_3 \times z) - C_5 \times \alpha_3 \times \sin(\alpha_3 \times z) - \frac{M}{l \times F} \\ y_3'' = -C_5 \times \alpha_3^2 \times \cos(\alpha_3 \times z) - C_6 \times \alpha_3^2 \times \sin(\alpha_3 \times z) \end{array} \right. \quad (16)$$

For the moment on support D attached to the second beam, the equations will take the form:

$$\left\{ \begin{array}{l} y_1 = C_1 \times \cos(\alpha_1 \times z) + C_2 \times \sin(\alpha_1 \times z) + \frac{M}{l \times F} \times z - \frac{M}{F}, \text{ where } 0 < z < k1l \\ y_1' = C_2 \times \alpha_1 \times \cos(\alpha_1 \times z) - C_1 \times \alpha_1 \times \sin(\alpha_1 \times z) + \frac{M}{l \times F} \\ y_1'' = -C_1 \times \alpha_1^2 \times \cos(\alpha_1 \times z) - C_2 \times \alpha_1^2 \times \sin(\alpha_1 \times z) \\ y_2 = C_3 \times \cos(\alpha_2 \times z) + C_4 \times \sin(\alpha_2 \times z) + \frac{M}{l \times F} \times z - \frac{M}{F}, \text{ where } k1l < z < k2l \\ y_2' = C_4 \times \alpha_2 \times \cos(\alpha_2 \times z) - C_3 \times \alpha_2 \times \sin(\alpha_2 \times z) + \frac{M}{l \times F} \\ y_2'' = -C_3 \times \alpha_2^2 \times \cos(\alpha_2 \times z) - C_4 \times \alpha_2^2 \times \sin(\alpha_2 \times z) \\ y_3 = C_5 \times \cos(\alpha_3 \times z) + C_6 \times \sin(\alpha_3 \times z) + \frac{M}{l \times F} \times z - \frac{M}{F}, \text{ where } k2l < z < l \\ y_3' = C_6 \times \alpha_3 \times \cos(\alpha_3 \times z) - C_5 \times \alpha_3 \times \sin(\alpha_3 \times z) + \frac{M}{l \times F} \\ y_3'' = -C_5 \times \alpha_3^2 \times \cos(\alpha_3 \times z) - C_6 \times \alpha_3^2 \times \sin(\alpha_3 \times z) \end{array} \right. \quad (17)$$

Using (14), (15), (16) and (17) we construct the diagrams of the moments (Fig. 12). Further, to determine the centers of mass, it is necessary to calculate the area of each of the Figs. (1-12) guided by the following rules:

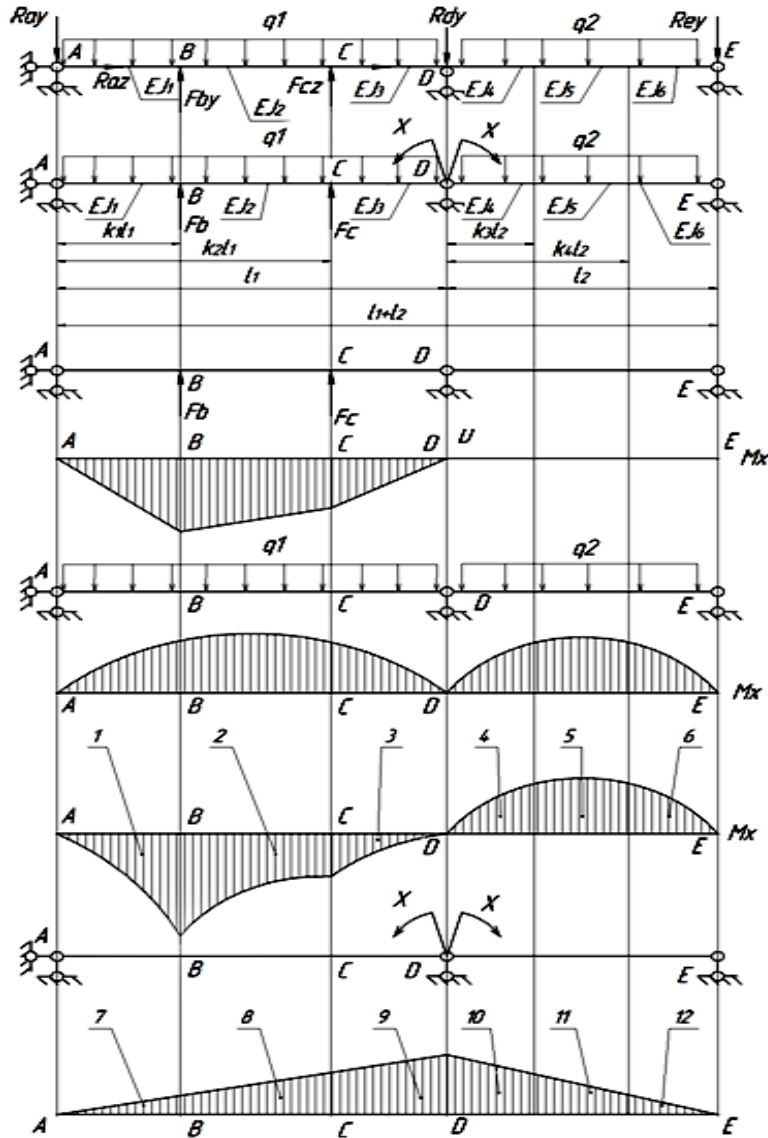


Fig. 12. Diagrams of the moment Calculation of the area of the basic loads diagram.

In general, the formula for calculating the area of an arbitrary shape is as follows:

$$S = \iint_D dzdy = \int_0^z dz \int_0^y dy = \int_0^z ydz$$

– For beam I:

1) $y_1^s = y_1^c + y_1^p$

$$S_1 = \int_0^{k_1 l} y_1^s dz = \int_0^{k_1 l} \left(C_1^p \times \alpha_1^2 \times \cos(\alpha_1 \times z) + C_2^p \times \alpha_1^2 \times \sin(\alpha_1 \times z) - C_2^c \times \alpha_1^2 \times \sin(\alpha_1 \times z) - \frac{q}{F} \right) dz =$$

$$= C_1^p \times \alpha_1 \times \sin(X_{11}) - \frac{q \times k_1 \times l}{F} - C_2^p \times \alpha_1 \times (\cos(X_{11}) - 1) + C_2^c \times \alpha_1 \times (\cos(X_{11}) - 1)$$

2) $y_2^s = y_2^c + y_2^p$

$$S_2 = \int_{k_1 l}^{k_2 l} y_2^s dz = \alpha_2 \times (C_3^p - C_3^c) \times (\sin(X_{22}) - \sin(X_{21})) + \alpha_2 \times (C_4^p - C_4^c) \times (\cos(X_{21}) - \cos(X_{22})) - \frac{q \times l \times (k_2 - k_1)}{F}$$

3) $y_3^s = y_3^c + y_3^p$

$$S_3 = \int_{k_2 l}^l y_3^s dz = \alpha_3 \times (C_5^p - C_5^c) \times (\sin(X_{30}) - \sin(X_{32})) + \alpha_3 \times (C_6^p - C_6^c) \times (\cos(X_{32}) - \cos(X_{30})) - \frac{q \times l \times (1 - k_2)}{F}$$

– For beam II:

4) $y_4^s = y_1^p$

$$S_4 = \int_0^{k_1 l} y_1^s dz = \int_0^{k_1 l} \left(C_1^p \times \alpha_1^2 \times \cos(\alpha_1 \times z) + C_2^p \times \alpha_1^2 \times \sin(\alpha_1 \times z) - \frac{q}{F} \right) dz =$$

$$= C_1^p \times \alpha_1 \times \sin(X_{11}) + C_2^p \times \alpha_1 \times (1 - \cos(X_{11})) - \frac{q \times k_1 \times l}{F}$$

$$5) y_5^s = y_2^p$$

$$S_5 = \int_{k_1 l}^{k_2 l} y_5^s dz = \alpha_2 \times C_3^p \times (\sin(X_{22}) - \sin(X_{21})) + \alpha_2 \times C_4^p \times (\cos(X_{21}) - \cos(X_{22})) - \frac{q \times l \times (k_2 - k_1)}{F}$$

$$6) y_6^s = y_3^p$$

$$S_6 = \int_{k_2 l}^l y_6^s dz = \alpha_3 \times C_5^p \times (\sin(X_{30}) - \sin(X_{32})) + \alpha_3 \times C_6^p \times (\cos(X_{32}) - \cos(X_{30})) - \frac{q \times l \times (1 - k_2)}{F}$$

Calculation of the area of the diagram of the moment on the support D:

— For beam I:

$$7) y_7^s = y_1^M$$

$$S_7 = \int_0^{k_1 l} y_7^s dz = C_1^M \times \alpha_1 \times \sin(X_{11}) + C_2^M \times \alpha_1 \times (1 - \cos(X_{11}))$$

$$8) y_8^s = y_2^M$$

$$S_8 = \int_{k_1 l}^{k_2 l} y_8^s dz = \alpha_2 \times C_3^M \times (\sin(X_{22}) - \sin(X_{21})) + \alpha_2 \times C_4^M \times (\cos(X_{21}) - \cos(X_{22}))$$

$$9) y_9^s = y_3^M$$

$$S_9 = \int_{k_2 l}^l y_9^s dz = \alpha_3 \times C_5^M \times (\sin(X_{30}) - \sin(X_{32})) + \alpha_3 \times C_6^M \times (\cos(X_{32}) - \cos(X_{30}))$$

— For beam II:

the formulas for the second beam are completely similar to the formulas for the first one.

Determination of the moment of inertia J_x of the diagrams of the main loads:

$$J_i^x = \iint_D z dz dy = \int_0^{k_1 l} z dz \int_0^y dy = \int_0^{k_1 l} (z \times y) dz$$

— For beam I:

$$1) y_1 = y_1^c + y_1^p$$

$$J_1^x = \int_0^{k_1 l} z \times (C_1^p \times \alpha_1^2 \times \cos(\alpha_1 \times z) + C_2^p \times \alpha_1^2 \times \sin(\alpha_1 \times z) - C_2^c \times \alpha_1^2 \times \sin(\alpha_1 \times z) - \frac{q}{F}) dz$$

$$= C_1^p \times (\cos(X_{11}) + \alpha_1 \times k_1 \times l \times \sin(X_{11}) - 1) + C_2^p \times (\sin(X_{11}) - \alpha_1 \times k_1 \times l \times \cos(X_{11})) - C_2^c$$

$$\times (\sin(X_{11}) - \alpha_1 \times k_1 \times l \times \cos(X_{11})) - \frac{q \times k_1^2 \times l^2}{2 \times F}$$

$$2) y_2 = y_2^c + y_2^p$$

$$J_2^x = \int_{k_1 l}^{k_2 l} z \times (C_3^p \times \alpha_2^2 \times \cos(\alpha_2 \times z) - C_3^c \times \alpha_2^2 \times \cos(\alpha_2 \times z) + C_4^p \times \alpha_2^2 \times \sin(\alpha_2 \times z) - C_4^c \times \alpha_2^2 \times \sin(\alpha_2 \times z) - \frac{q}{F}) dz$$

$$= (C_3^p - C_3^c) \times (\cos(X_{22}) - \cos(X_{21}) + \alpha_2 \times l \times (k_2 \times \sin(X_{22}) - k_1 \times \sin(X_{21}))) + (C_4^p - C_4^c)$$

$$\times (\sin(X_{22}) - \sin(X_{21}) + \alpha_2 \times l \times (k_1 \times \cos(X_{21}) - k_2 \times \cos(X_{22}))) - \frac{q \times l^2 \times (k_2^2 - k_1^2)}{2 \times F}$$

$$3) y_3 = y_3^c + y_3^p$$

$$J_3^x = \int_{k_2 l}^l z \times (C_5^p \times \alpha_3^2 \times \cos(\alpha_3 \times z) + C_6^p \times \alpha_3^2 \times \sin(\alpha_3 \times z) - C_5^c \times \alpha_3^2 \times \cos(\alpha_3 \times z) - C_6^c \times \alpha_3^2 \times \sin(\alpha_3 \times z) - \frac{q}{F}) dz$$

$$= (C_5^p - C_5^c) \times (\cos(X_{30}) - \cos(X_{32}) + \alpha_3 \times l \times (\sin(X_{30}) - k_2 \times \sin(X_{32}))) - (C_6^p - C_6^c)$$

$$\times (\sin(X_{30}) - \sin(X_{32}) + \alpha_3 \times l \times (k_2 \times \cos(X_{32}) - \cos(X_{30}))) - \frac{q \times l^2 \times (1 - k_2^2)}{2 \times F}$$

— For beam II:

$$4) y_4 = y_1^p$$

$$J_4^x = \int_0^{k_1 l} z \times (C_1^p \times \alpha_1^2 \times \cos(\alpha_1 \times z) + C_2^p \times \alpha_1^2 \times \sin(\alpha_1 \times z) - \frac{q}{F}) dz$$

$$= C_1^p \times (\cos(X_{11}) + \alpha_1 \times k_1 \times l$$

$$\times \sin(X_{11}) - 1) + C_2^p \times (\sin(X_{11}) + \alpha_1 \times k_1 \times l \times \cos(X_{11})) - \frac{q \times k_1^2 \times l^2}{2 \times F}$$

$$5) y_5 = y_2^p$$

$$J_5^x = \int_{k_1 l}^{k_2 l} z \times (C_3^p \times \alpha_2^2 \times \cos(\alpha_2 \times z) + C_4^p \times \alpha_2^2 \times \sin(\alpha_2 \times z) - \frac{q}{F}) dz$$

$$= C_3^p \times (\cos(X_{22}) - \cos(X_{21}) + \alpha_2 \times l$$

$$\times (k_2 \times \sin(X_{22}) - k_1 \times \sin(X_{21}))) + C_4^p \times (\sin(X_{22}) - \sin(X_{21}) + \alpha_2 \times l \times (k_1 \times \cos(X_{21}) - k_2$$

$$\times \cos(X_{22}))) - \frac{q \times l^2 \times (k_2^2 - k_1^2)}{2 \times F}$$

$$6) y_6 = y_3^p$$

$$J_6^X = \int_{k_{2l}}^l z \times (C_5^p \times \alpha_3^2 \times \cos(\alpha_3 \times z) + C_6^p \times \alpha_3^2 \times \sin(\alpha_3 \times z) - \frac{q}{F}) dz$$

$$= \frac{C_5^p \times (\cos(X_{30}) - \cos(X_{32}) + \alpha_3 \times l \times (\sin(X_{30}) - k_2 \times \sin(X_{32}))) + C_6^p \times (\sin(X_{30}) - \sin(X_{32}) + \alpha_3 \times l \times (k_2 \times \cos(X_{32}) - \cos(X_{30}))) - \frac{q \times l^2 \times (1 - k_2^2)}{2 \times F}}$$

Determination of the moment of inertia Jx of the diagram on support D

– For beam I:

$$7) y_7 = y_1^M$$

$$J_7^X = \int_0^{k_{1l}} z \times (C_1^M \times \alpha_1^2 \times \cos(\alpha_1 \times z) + C_2^M \times \alpha_1^2 \times \sin(\alpha_1 \times z)) dz = C_1^M \times (\cos(X_{11}) + \alpha_1 \times k_1 \times l \times (\sin(X_{11}) - 1))$$

$$8) y_8 = y_2^M$$

$$J_8^X = \int_{k_{1l}}^{k_{2l}} z \times (C_3^M \times \alpha_2^2 \times \cos(\alpha_2 \times z) + C_4^M \times \alpha_2^2 \times \sin(\alpha_2 \times z)) dz$$

$$= C_3^M \times (\cos(X_{22}) - \cos(X_{21}) + \alpha_2 \times l \times (k_2 \times \sin(X_{22}) - k_1 \times \sin(X_{21}))) + C_4^M \times (\sin(X_{22}) - \sin(X_{21}) + \alpha_2 \times l \times (k_1 \times \cos(X_{21}) - k_2 \times \cos(X_{22})))$$

$$9) y_9 = y_3^M$$

$$J_9^X = \int_{k_{2l}}^l z \times (C_5^M \times \alpha_3^2 \times \cos(\alpha_3 \times z) + C_6^M \times \alpha_3^2 \times \sin(\alpha_3 \times z)) dz$$

$$= C_5^M \times (\cos(X_{30}) - \cos(X_{32}) + \alpha_3 \times l \times (\sin(X_{30}) - k_2 \times \sin(X_{32}))) + C_6^M \times (\sin(X_{30}) - \sin(X_{32}) + \alpha_3 \times l \times (k_2 \times \cos(X_{32}) - \cos(X_{30})))$$

— For beam II:

the formulas for the second beam are completely similar to the formulas for the first one.

Further, to find the center of mass, it is necessary to divide the moment of inertia of the corresponding section of the diagram into its area:

$$z_i = \frac{J_i^X}{S_i} \quad (18)$$

It is necessary to put the obtained values in (14), (15), (16) and (17) and determine the values of the moments at these points, then use (11) to calculate the unknown moment. After defining the moment on the middle support, it is easy to calculate the reactions on the extreme supports A and E.

The lateral reaction on support A is the desired deflecting lateral force on the bit, which determines the intensity of milling of the bore hole wall.

III. RESULTS AND DISCUSSION

As a result of the work carried out in this article, relations have been obtained that allow us to determine the forces acting directly on the bit while drilling with the use of the RSS. The application of the developed mathematical model will allow analyzing and predicting the parameters of the rock destruction process using modern polycrystalline diamond compact bits in conjunction with a small diameter RSS.

The presented mathematical model of the BHA with RSS allows determining the main operational characteristics of the RSS to ensure a reliable process of steerable drilling.

The capabilities provided by this model are especially important for the further analysis of the design features of the developed small-diameter RSS (4.75 inches outer diameter and less), which require an accurate calculation of drill string forces in the case of limited dimensions of the structural elements.

The development and study of the principles of controlling the trajectory curvature vector when drilling small diameter wells using RSS consists primarily in creating a constructive product concept consisting of a choice of layout, method of controlling this layout and functional features inherent in each particular implementation. In addition to developing the concept itself, special attention should be paid to the method of integrating the product into the BHA [16], in terms of mechanical docking and the implementation of the communication channel with the MWD system.

As a result of the studies, a comprehensive approach to the design of a small-diameter rotary controlled system based on the use of standard replacement elements as components of the product has been proposed.

IV. CONCLUSION AND FUTURE SCOPE

In the future, this study may help in the development of a wide range of RSS, in particular - the most important for the industry - small diameter systems. The main area of future research is the solution of conceptual issues of the structural layout of the RSS, as well as the formulation and solution of problems of algorithmic optimization of the directional drilling process.

ACKNOWLEDGEMENT

The project is being implemented by Federal State Autonomous Educational Institution for Higher Education "Peter the Great St. Petersburg Polytechnic University" together with an industrial partner of Special Design Bureau of Underground Navigation Devices JSC. The commissioner is the Ministry of Education and Science of the Russian Federation. Project Theme: "Development and research of the principles of trajectory curvature vector control when drilling small diameter wells using rotary steerable systems" (Agreement No.075-15-2019-1403 of June 20, 2019 UIP RFMEFI57517X0138). This project is being implemented with financial support from the Ministry of Education and Science of the Russian Federation.

Conflict of interest. The authors declare no conflict of interest.

REFERENCES

- [1]. Ovchinnikov V. P., Dvojniov M. V., Gerasimov G. T., Ivancov A. Ju. (2008). Technologies And technological means of drilling curved wells. Textbook for universities [Technologies and technological tools for drilling the inclined wells. Textbook for high schools.]. Tjumen': Izd-voTjumGNGU.
- [2]. Elshafei, M., Khaim, M., & Al-Majed, A. (2015). Optimization of rotary steerable drilling. *Proceedings of the 2nd International Conference of Control, Dynamic Systems, and Robotics*. Ottawa, Ontario, Canada, May 7-8, 167.
- [3]. Xinjuna, G., & Jinga, L. (2014). Research on application of steering drilling technologies in shale gas development. *Geological Engineering Drilling Technology Conference (IGEDTC)*, New International
- [4]. Convention Exposition Center Chengdu Century City on 23rd-25th, 270-275.
- [5]. Suslick, S. B., & Schiozer, D. J. (2004). Risk analysis to petroleum exploration and production: an overview. *Journal of petroleum science and engineering*, 44(2), 1-9.
- [6]. Wenhui, Y., Yong, P., Shaohuai, Zh., & Heng, W. (2016). Research on rotary steerable drilling system. *Metallurgical and mining industry*, 2, 144-148.
- [7]. Wang, W., Geng, Ya., Wang, N., Pu, X., & Fiaux J. O. (2019). Toolface control method for a dynamic point-the-bit rotary steerable drilling system. *Energies*, 12(10): 18-31.
- [8]. Kalinin, A. G., Nikitin, B. A., Solodkij, K. M., & Sultanov, B. Z. (1997). Drilling of deviated and horizontal wells: Reference [Drilling of inclined and horizontal wells: Handbook]. Moscow: Nedra.
- [9]. Dvojniov, M. V. (2017). Analysis of research results of technical and technological parameters of drilling deviated wells [Analysis of the results of studies of technical and technological parameters of drilling the inclined wells]. *Zapiski Gornogoinstituta*, 223: 86-92.
- [10]. Wang, H., Guan Zh. C., Shi, Yu. C., & Liang, De. Ya. (2017). Study on Build-up Rate of Push-the-bit Rotary Steerable Bottom Hole Assembly. *Journal of Applied Science and Engineering*, 20(3): 401-408.
- [11]. Ashcheulov, A., & Nikitin, S. (2018). Dynamic Model of a Drilling Rig with a Top Drive System for Rotary Steerable Systems. *International Journal of Engineering & Technology*, 7(4.28): 1574-1579.
- [12]. Tkachenko, V. V., Lukyanenko, T. V., & Shadrina, Zh. A. (2019). A Set of Economic and Mathematical Models for Assessment of Agricultural Crop Cultivation Technologies. *International Journal of Recent Technology and Engineering*, 2(2): 3829-3833.
- [13]. Kiseleva, I. A., Kuznetsov V. I., Sadovnikova, N. A., Chernysheva, E. N., Androshina, I. S. (2019). Mathematical Modeling of Investment Risks. *International Journal of Innovative Technology and Exploring Engineering*, 8(7): 2376-2379.
- [14]. Dudin, M. N., Lyasnikov, N. V., Katul'skiy, E. D., Shhipanova, D. G., & Chekanov, A. E. (2017). Diversified Approach to Quantification of Risks that Arise in Projects Associated with Extraction of Hydrocarbon Resources in the Arctic. *Journal of Environmental Management and Tourism*, 8(1): 31-44.
- [15]. Gaisina, L. M., Belonozhko, M. L., Kirichuk, S. M., Sultanova, E. A., & Tumanova, A. Y. (2017). Self-organization and Self-development as Key Factors in Improving Productivity. *Journal of Advanced Research in Law and Economics*, 8(2): 444-453.
- [16]. Klimov, A.S. (2015). Improving the efficiency of drilling directional and horizontal wells// Compilation of scientific articles IRNTU: 27.

How to cite this article: Binder, Y. I., Kharlamova, E. E., Kharlamov, V. E., Lozhechko, V. P., Smirnov, V. A. and Sokolov, D. A. (2019). Development of Mathematical Model of Bottom Hole Assembly for Rotary Steerable System. *International Journal on Emerging Technologies*, 10(4): 422-433.